

Non-classical two-photon interference between independent telecom light pulses converted by difference-frequency generation

Rikizo Ikuta,¹ Toshiki Kobayashi,¹ Hiroshi Kato,¹ Shigehito Miki,² Taro Yamashita,² Hiroataka Terai,² Mikio Fujiwara,³ Takashi Yamamoto,¹ Masato Koashi,⁴ Masahide Sasaki,³ Zhen Wang,² and Nobuyuki Imoto¹

¹Graduate School of Engineering Science, Osaka University, Toyonaka, Osaka 560-8531, Japan

²Advanced ICT Research Institute, National Institute of Information and Communications Technology (NICT), Kobe 651-2492, Japan

³Advanced ICT Research Institute, National Institute of Information and Communications Technology (NICT), Koganei, Tokyo 184-8795, Japan

⁴Photon Science Center, The University of Tokyo, Bunkyo-ku, 113-8656, Japan

We experimentally demonstrated the Hong-Ou-Mandel (HOM) interference between two photons after visible-to-telecommunication wavelength conversion. In the experiment, we prepared a heralded single photon by using spontaneous parametric down-conversion and the other photon from a weak laser source at 780 nm. We converted the wavelength of both photons to the telecommunication wavelength of 1522 nm by using difference-frequency generation in a periodically-poled lithium niobate, and then observed the HOM interference between the photons. The observed visibility is 0.76 ± 0.12 which clearly shows the non-classical interference of the two photons. The high-visibility interference is an important step for fiber-based quantum communications of photons generated from visible photon emitters.

PACS numbers: 03.67.Hk, 42.65.Ky, 42.50.Dv, 42.50.Ex

Quantum interface for wavelength conversion of photons [1] is an important building block for linking quantum information among different kinds of physical systems, and it has been actively studied [2–11]. Especially, for optical-fiber-based quantum communication over a long distance with quantum repeaters [12], wavelength conversion of photons entangled with quantum memories to telecommunication bands without destroying their quantum information is required. Many promising quantum memories have resonant wavelengths at the visible range [13–19], which necessitates a quantum interface for visible-to-telecommunication wavelength conversion. Furthermore, in order to establish an entanglement between the remote quantum memories through two-photon interference [19–24], two down-converted telecom photons should be detected by the Bell measurement (BM) at the intermediate relay node, as illustrated in Fig. 1. In the BM, the two telecom photons must be indistinguishable, and cause non-classical interference, i.e. the Hong-Ou-Mandel (HOM) interference [25]. Entanglement-preserving visible-to-telecommunication wavelength conversions have been demonstrated in [6, 7, 9], and highly entangled states have been observed [6, 9]. However, the HOM interference at the relay node has never been demonstrated. Related experiments have been restricted to the HOM interference between up-converted visible photons [3, 11].

In this Letter, we present the first demonstration of the HOM interference between two light pulses at the telecommunication band after frequency down-conversion, which matches up with fiber-based quantum communication with quantum repeaters. We initially prepared two pulses at 780 nm, one being a heralded

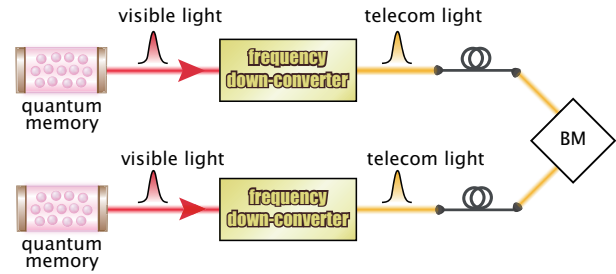


FIG. 1: An elementary link of quantum repeaters with the quantum interface. Each quantum memory has two excitation modes coupled to two modes of a photon such as polarization. Visible photons entangled with quantum memories are frequency down-converted to the telecommunication bands, and pass through optical fibers. The Bell measurement is performed on the two photons for establishing entanglement between the quantum memories.

single photon generated from spontaneous parametric down-conversion (SPDC) and the other being a coherent light pulse directly from the laser. Their wavelengths were converted to 1522 nm by difference-frequency generation (DFG) using a periodically-poled LiNbO₃ (PPLN) waveguide. We then observed the HOM interference between the converted light pulses. The interference visibility was 0.76 ± 0.12 , which clearly exceeds the maximum value of 0.5 in the classical wave theory [26]. A comparison to our theoretical analysis shows that the degradation of the visibility is mainly caused by the multi-photon events from the coherent light pulse, which suggests that the demonstrated frequency down-converter will enable us to achieve a visibility as high as 0.91.

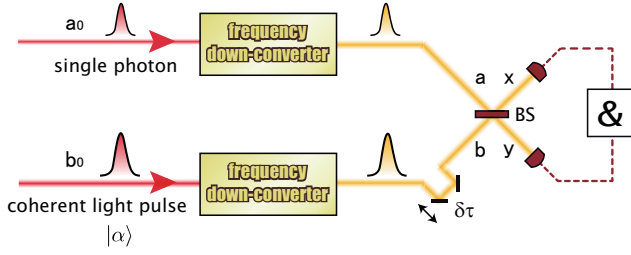


FIG. 2: Concept of our experimental setup. A single photon is prepared by measuring one of the photon pair from the SPDC. The coherent light pulse is prepared by the laser source.

A conceptual setup of the HOM interference after the wavelength conversion in our experiment is shown in Fig. 2. The two input visible light pulses are a coherent light pulse and a heralded single photon. The two pulses have no correlations and they are regarded as prepared from independent sources [27–29]. The two visible light pulses are frequency down-converted to the telecommunication wavelength, and then they are combined by a half beamsplitter (BS). When the photons from the two pulses are indistinguishable, they always leave the same output port of the BS. On the other hand, the photons may appear in both output ports if these are not completely indistinguishable. By measuring the coincidence photon detection between the two output modes of the BS while changing the time delay $\delta\tau$ between the two light pulses, we observe the HOM dip. In the classical wave theory, the maximum of the visibility of the HOM interference is 0.5.

The experimental setup for the HOM interference is shown in Fig. 3 (a). A pico-second light pulse from a mode-locked Ti:sapphire (Ti:S) laser (wavelength: 780 nm; pulse width: $\Delta t \equiv 1.2$ ps; repetition rate: 82 MHz) is divided into two beams. One beam is frequency doubled (wavelength: 390 nm; power: 200 mW) by second harmonic generation (SHG), and then pumps a Type-I phase-matched 1.5mm-thick β -barium borate (BBO) crystal to generate a vertically(V)-polarized photon pair in modes A and B through SPDC. The photon in mode A is measured by a superconducting single photon detector (SSPD) [31, 32] denoted by D_V for preparing a heralded single photon in mode B. The spectral filtering of the photon in mode A is performed by a Bragg grating (BG1) with a bandwidth of $\Delta_{BG1} \equiv 0.2$ nm. The other beam is weakened to an average photon number of ~ 0.5 by using a glass plate (GP), and is sent along the same light path as the photon B. Time difference between the photon B and the subsequent coherent light pulse is set to be ~ 400 ps which is longer than the temporal resolution 150 ps of the detectors [9]. The two light pulses in the visible range are then sent to the frequency down-converter.

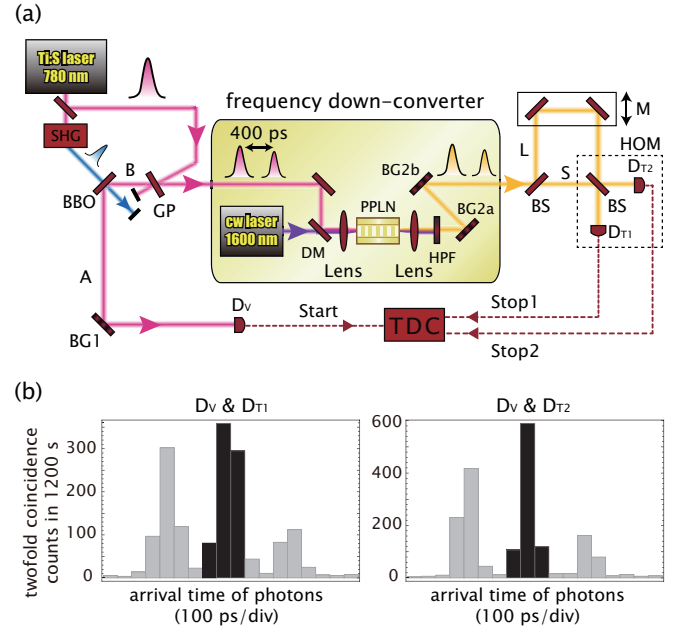


FIG. 3: (a) The experimental setup for the HOM interference after the wavelength conversion. The single PPLN waveguide is used for the wavelength conversion of the heralded single photon and the coherent light pulse. (b) Twofold coincidence counts between D_V and D_{T1} , and between D_V and D_{T2} . In each histogram, three peaks of the arrival time of the stop signal are observed. For the threefold coincidence events among D_V , D_{T1} and D_{T2} , we post-select the 300-ps time windows of the two central peaks.

In the frequency down-converter, a V-polarized cw pump laser at 1600 nm with an effective power of 500 mW is combined with the signal beams at 780 nm by a dichroic mirror (DM). They are focused on the Type-0 quasi-phase matched PPLN waveguide [30]. The length of the PPLN crystal is 20 mm and the acceptable bandwidth is calculated to be $\Delta_{WG} \equiv 0.3$ nm. After passing through the PPLN waveguide, the strong pump light is reduced by a high-pass filter (HPF), and the light converted to the wavelength of 1522 nm is extracted by BG2a and BG2b with bandwidths of $\Delta_{BG2} \equiv 1$ nm.

The light pulses from the frequency down-converter are split into a short path (S) and a long path (L) by a BS. Time difference between S and L is changed by mirrors (M) on a motorized stage. The pulses passing through S and L are mixed by a second BS for the HOM interference. The two output beams from the BS are coupled to single-mode fibers followed by two SSPDs D_{T1} and D_{T2} .

An electric signal from D_V is connected to a time-to-digital converter (TDC) as a start signal of a clock, and electric signals from D_{T1} and D_{T2} are connected to the TDC as stop signals. Fig. 3 (b) shows the histograms of the delayed coincidence counts of $D_V \& D_{T1}$ and $D_V \& D_{T2}$. The central peak among the observed three peaks in each

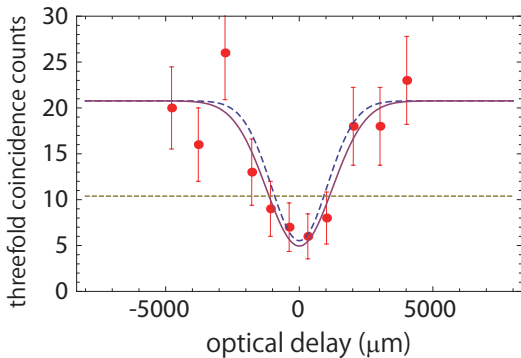


FIG. 4: Observed HOM interference between two light pulses. The threefold coincidence counts have been observed in the 300-ps time windows. Solid curves are Gaussian fitted to the experimental counts. Dashed curves are obtained by Eq. (4) with experimental parameters. Dashed horizontal lines describe the minimum values of the dips in the classical wave theory.

histogram includes the events where two photons simultaneously arrived at the BS, i.e., the heralded single photon passed through path L and the coherent light pulse passed through path S. Therefore, to see the HOM interference, we collect the coincidence events within 300-ps time windows of the two central peaks, which corresponds to the threefold coincidence events among D_V , D_{T1} and D_{T2} . We note that while the duration of the converted light pulse is ~ 5 ps, the observed widths of the peaks shown in Fig. 3 (b) are much larger, coming from the timing resolution of our measurement system. The 300-ps time window was chosen such that the tails of the left and right peaks are negligible.

The experimental result of the dependency of the threefold coincidence counts on the optical delay is shown in Fig. 4, which clearly indicates the HOM dip. Each point was recorded for 23 hours. The observed visibility of 0.76 ± 0.12 at the zero delay point was obtained by the best fit to the experimental data with a Gaussian. The full width at half maximum was approximately 2.9 nm which corresponds to ~ 10 ps for a delay time. The high visibility clearly shows the non-classical interference of the two light pulses converted to the telecommunication band.

To see the reasons for the degradation of the visibility, we construct a theoretical model which takes into account the mode mismatch between the two pulses, and vacuum and multi-photon components in the coherent light pulse. The emission rate of the photon pair from the SPDC is so small that the multiple-pair events are negligible in our experiment. In addition, the heralded single photon is assumed to be in a pure state because the narrow-band spectral filtering destroys the spectral correlation between the photon pairs from SPDC. Under the assumptions, the initial state composed of the single

photon in mode a_0 and the light in the coherent state in mode b_0 , which are shown in Fig. 2, is regarded as a pure state described by $\hat{a}_{a_0}^\dagger \hat{D}_{b_0}(\alpha)|0\rangle$, where $|0\rangle$ is the vacuum state for both paths, \hat{a}^\dagger is a bosonic creation operator and $\hat{D}_{b_0}(\alpha) \equiv \exp(\alpha \hat{a}_{b_0}^\dagger - \alpha^* \hat{a}_{b_0})$ with complex number α is a displacement operator. The subscripts denote the modes on which the operators work.

In the experiment for the HOM interference, the two light pulses are mixed at the BS and detected by threshold photon detectors which cannot distinguish the photon numbers and which have the same quantum efficiency denoted by η . Such a measurement is equivalent to photon detections with unit efficiency after the lights pass through a lossy channel with transmittance η and then they are mixed by the BS [33]. As a result, by using effective overall transmittance T which includes all of the photonic losses in the circuit such as the conversion efficiency of the frequency down-converter and the quantum efficiency of the detector, the input state of the light pulses in modes a and b to the BS is regarded as $|\phi_T\rangle \equiv \hat{a}_a^\dagger \hat{D}_b(\sqrt{T}\alpha)|0\rangle$ with probability T and as $|\phi_R\rangle \equiv \hat{D}_b(\sqrt{T}\alpha)|0\rangle$ with probability $1 - T$.

Two light pulses in modes a and b are mixed at the BS and channeled into paths x and y . Suppose that mode a is transformed into modes x_a and y_a , and mode b is transformed into modes x_b and y_b . The overlap between modes x_a and x_b (y_a and y_b) represented by $V \equiv |[\hat{a}_{x_a}, \hat{a}_{x_b}^\dagger]|^2 = |[\hat{a}_{y_a}, \hat{a}_{y_b}^\dagger]|^2$ depends on the time delay $\delta\tau$, and it may not be unity even for $\delta\tau = 0$ due to the mismatch in the spectral shapes of the pulses. When the normalized spectral amplitudes of modes a and b are assumed to be Gaussian with variances of $\delta\omega_p^2$ and $\delta\omega_w^2$ respectively, the overlap V is given by

$$V(\delta\tau) = \left| \frac{1}{\sqrt{\pi\delta\omega_p\delta\omega_w}} \int e^{-i\omega\delta\tau} e^{-\frac{\omega^2}{2\delta\omega_p^2}} e^{-\frac{\omega^2}{2\delta\omega_w^2}} d\omega \right|^2 \quad (1)$$

$$= \frac{2\delta\omega_p\delta\omega_w}{\delta\omega_p^2 + \delta\omega_w^2} \exp\left[-\frac{\delta\omega_p^2\delta\omega_w^2\delta\tau^2}{\delta\omega_p^2 + \delta\omega_w^2} \right]. \quad (2)$$

In our experiment, by using $\Delta t = 1.2$ ps, $\Delta_{BG1} = 0.2$ nm, $\Delta_{WG} = 0.3$ nm and $\Delta_{BG2} = 1$ nm which are the full widths at the half maxima, and by assuming that all spectral functions are Gaussian, $V(0)$ is calculated to be larger than 0.99.

We also take into account the effect of background noises which include the Raman scattering of the cw pump light and the dark counts of the detectors. While the optical noise caused by the Raman scattering may interfere with the pico-second signal photons, such contribution is negligible in the 300-ps time window. We thus model the effect of these noises as a single parameter d , such that each of detectors signals a detection with probability d even when no photons are incident. The twofold coincidence probability between the light pulses

after the BS is described by

$$P(\delta\tau) = TP_T(\delta\tau) + (1 - T)P_R, \quad (3)$$

where $P_T(\delta\tau) \equiv 1 - (1 - d)(\|\langle 0|_x \hat{U}|\phi_T\rangle\|^2 + \|\langle 0|_y \hat{U}|\phi_T\rangle\|^2)$ and $P_R \equiv 1 - (1 - d)(\|\langle 0|_x \hat{U}|\phi_R\rangle\|^2 + \|\langle 0|_y \hat{U}|\phi_R\rangle\|^2) - (1 - d)\langle 0|_x \langle 0|_y \hat{U}|\phi_R\rangle|^2$. $|0\rangle_i$ represents the vacuum state of path i . \hat{U} is a unitary operator for the action of the BS, and it satisfies $\hat{U}\hat{a}_a^\dagger\hat{U}^\dagger = (\hat{a}_{x_a}^\dagger - \hat{a}_{y_a}^\dagger)/\sqrt{2}$, $\hat{U}\hat{D}_b(\sqrt{T}\alpha)\hat{U}^\dagger = \hat{D}_{x_b}(\sqrt{T/2}\alpha)\hat{D}_{y_b}(\sqrt{T/2}\alpha)$ and $\hat{U}|0\rangle = |0\rangle_x|0\rangle_y$. By using $|\langle 0|_i \hat{D}_{i_b}(\sqrt{T/2}\alpha)|0\rangle_i|^2 = \exp(-T|\alpha|^2/2)$ and $\langle 0|_i \hat{D}_{i_b}^\dagger(\sqrt{T/2}\alpha)\hat{a}_{i_a}\hat{a}_{i_a}^\dagger\hat{D}_{i_b}(\sqrt{T/2}\alpha)|0\rangle_i = V(\delta\tau)T|\alpha|^2/2 + 1$ for $i = x, y$, we have

$$P(\delta\tau) \propto 1 - \frac{V(\delta\tau)}{\left(1 + \frac{2d}{T|\alpha|^2}\right)\left(1 + \frac{d}{T} + \frac{|\alpha|^2}{2}\right)}, \quad (4)$$

under the condition that $T \ll 1$ and $d \ll 1$ are satisfied. From Eq. (4), we see that the denominator consists of two factors originating from the vacuum component and the multi-photon components in the coherent state. As a result, there is an optimal value of $|\alpha|^2$ for minimizing $P(0)$. Using Eq. (4) and the observed parameters as $T \approx 0.0008$ and $d \approx 1.9 \times 10^{-5}$, the optimal value becomes $|\alpha|^2 \approx 0.31$. In our experiment, we chose $|\alpha|^2 \approx 0.43$ which implies that the contribution from the multi-photons is larger.

By using our experimental parameters, we plotted a curve predicted by the theoretical model written in Eq. (4). The curve is in good agreement with the experimental result. In our model, the main reason for the degradation of the visibility is estimated to be the effect of the multi-photons in the coherent light pulse, and thus the demonstrated frequency down-converter is expected to have small adverse effects in the interference. If we replace the coherent light pulse by a heralded single photon prepared similarly to the mode B in Fig. 3, the visibility of the two-photon interference will become 0.91 as a result of the above analysis. Such a situation is more compatible with the conceptual setup in Fig. 1.

In conclusion, we have demonstrated the HOM interference of the two light pulses which are frequency down-converted to the telecommunication wavelength of 1522 nm from the visible wavelength of 780 nm. We observed a visibility of 0.76 ± 0.12 , which clearly shows the non-classical interference of the two light pulses. The theoretical analysis indicates that the degradation of the visibility is mainly caused by the multi-photons in the coherent light pulse, and the visibility expected when we use heralded single photons for the photon sources is 0.91. We believe that the high-visibility wavelength conversion will be one of the key devices for many applications of quan-

tum communication over long distance such as quantum repeaters.

This work was supported by the Funding Program for World-Leading Innovative R & D on Science and Technology (FIRST), MEXT Grant-in-Aid for Scientific Research on Innovative Areas 20104003 and 21102008, the MEXT Global COE Program, and MEXT Grant-in-Aid for Young scientists(A) 23684035.

REFERENCES

- [1] P. Kumar, *Opt. Lett.* **15**, 1476 (1990).
- [2] S. Tanzilli *et al.* *Nature (London)* **437**, 116 (2005).
- [3] H. Takesue, *Phys. Rev. Lett.* **101**, 173901 (2008).
- [4] M. T. Rakher, L. Ma, O. T. Slattey, X. Tang, and K. A. Srinivasan, *Nature Photonics* **4**, 786 (2010).
- [5] H. J. McGuinness, M. G. Raymer, C. J. McKinstrie, and S. Radic, *Phys. Rev. Lett.* **105**, 093604 (2010).
- [6] Y. O. Dudin *et al.* *Phys. Rev. Lett.* **105**, 260502 (2010).
- [7] R. Ikuta *et al.*, *Nature Commun.* **2**, 537 (2011).
- [8] S. Ramelow, A. Fedrizzi, A. Poppe, N. K. Langford, and A. Zeilinger, *Phys. Rev. A* **85**, 013845 (2012).
- [9] R. Ikuta *et al.*, *Phys. Rev. A* **87**, 010301(R) (2013).
- [10] S. Zaske *et al.*, *Phys. Rev. Lett.* **109**, 147404 (2012).
- [11] S. Ates *et al.*, *Phys. Rev. Lett.* **109**, 147405 (2012).
- [12] N. Sangouard, C. Simon, H. de Riedmatten, and N. Gisin, *Rev. Mod. Phys.* **83**, 33 (2011).
- [13] D. N. Matsukevich, and A. Kuzmich, *Science* **306**, 663-666 (2004).
- [14] W. Rosenfeld *et al.*, *Phys. Rev. Lett.* **101**, 260403 (2008).
- [15] C. W. Chou *et al.*, *Nature (London)* **438**, 828 (2005).
- [16] S. Olmschenk *et al.*, *Science* **323**, 486 (2009).
- [17] E. Togan *et al.*, *Nature (London)* **466**, 730 (2010).
- [18] S. Ritter *et al.*, *Nature (London)* **484**, 195 (2012).
- [19] J. Hofmann *et al.*, *Science* **337**, 72 (2012).
- [20] J. Beugnon *et al.*, *Nature (London)* **440**, 779 (2006).
- [21] P. Maunz *et al.*, *Nature Physics* **3**, 538 (2007).
- [22] D. L. Moehring *et al.*, *Nature (London)* **449**, 68 (2007).
- [23] H. Bernien *et al.*, *Phys. Rev. Lett.* **108**, 043604 (2012).
- [24] A. Sipahigil *et al.*, *Phys. Rev. Lett.* **108**, 143601 (2012).
- [25] C. K. Hong, Z. Y. Ou, and L. Mandel, *Phys. Rev. Lett.* **59**, 2044 (1987).
- [26] Z. -Y. J. Ou, *Multi-photon Quantum Interference* (Springer, New York, 2007).
- [27] J. G. Rarity, P. R. Tapster, and R. Loudon, arXiv: quant-ph/9702032 (1997).
- [28] J. G. Rarity, P. R. Tapster, and R. Loudon, *J. Opt. B* **7**, S171 (2005).
- [29] R. -B. Jin *et al.*, *Phys. Rev. A* **83**, 031805(R) (2011).
- [30] T. Nishikawa *et al.*, *Opt. Express* **17**, 17792 (2009).
- [31] S. Miki, M. Takeda, M. Fujiwara, M. Sasaki, and Z. Wang, *Opt. Express* **17**, 23558 (2009).
- [32] S. Miki, T. Yamashita, M. Fujiwara, M. Sasaki, and Z. Wang, *Opt. Lett.* **35**, 2133 (2010).
- [33] M. Koashi, *Phys. Rev. Lett.* **93**, 120501 (2004).